JAAS

Accepted Manuscript

This article can be cited before page numbers have been issued, to do this please use: L. E. Morgan, D. P. Santiago Ramos, B. DAVIDHEISER-KROLL, J. Faithfull, N. S. Lloyd, R. Ellam and J. A. Higgins, *J. Anal. At. Spectrom.*, 2017, DOI: 10.1039/C7JA00257B.

ROYAL SOCIETY OF CHEMISTRY

rsc.li/jaas

View Article Online
DOI: 10.1039/C7JA00257B

High-precision $^{41}K/^{39}K$ measurements by MC-ICP-MS indicate terrestrial variability of $\delta^{41}K$

Leah E. Morgan[1,*], Danielle P. Santiago Ramos[2], Brett Davidheiser-Kroll[3], John Faithfull[4], Nicholas S. Lloyd[5], Rob M. Ellam[6], John A. Higgins[2]

[1]U.S. Geological Survey, Denver Federal Center, MS 963, Denver, CO 80225, USA
[2]Department of Geosciences, Princeton University, Princeton, NJ 08544, USA
[3]University of Colorado at Boulder, Boulder CO 80309, USA
[4]Hunterian Museum, University of Glasgow, University Ave., Glasgow, G12 8QQ, UK
[5]ThermoFisher Scientific, Hanna-Kunath-Str. 11, 28199 Bremen, Germany
[6]Scottish Universities Environmental Research Centre, Rankine Ave., East Kilbride, G75 0QF, UK

*corresponding author email: lemorgan@usgs.gov

Abstract

Potassium is a major component in continental crust, the fourth-most abundant cation in seawater, and a key element in biological processes. Until recently, difficulties with existing analytical techniques hindered our ability to identify natural isotopic variability of potassium isotopes in terrestrial materials. However, measurement precision has greatly improved, and a range of K isotopic compositions has now been demonstrated in natural samples. In this study, we present a new technique for high-precision measurement of K isotopic ratios using high-resolution, cold plasma multi-collector mass spectrometry. We apply this technique to demonstrate natural variability in the ratio of ^{41}K to ^{39}K in a diverse group of geological and biological samples, including silicate and evaporite minerals, seawater, and plant and animal tissues. The total range in $^{41}K/^{39}K$ ratios is ca. 2.6‰, with a long-term external reproducibility of 0.17‰ (2σ, N=108). Seawater and seawater-derived evaporite minerals are systematically enriched in ^{41}K compared to silicate minerals by ca. 0.6‰, a result consistent with recent findings[1, 2]. Although our average bulk-silicate Earth value (-0.54‰) is indistinguishable from previously published values, we find systematic $\delta^{41}K$ variability in some high-temperature sample suites, particularly those with evidence for the presence of fluids. The $\delta^{41}K$ values of biological samples span a range of ca. 1.2‰ between terrestrial mammals, plants, and marine organisms. Implications of terrestrial K isotope variability for the atomic weight of K and K-based geochronology are discussed. Our results

View Article Online
DOI: 10.1039/C7JA00257B

indicate that high-precision measurements of stable K isotopes, made using commercially available mass spectrometers, can provide unique insights into the chemistry of potassium in geological and biological systems.

1. Introduction

Potassium is a major element in continental crust, a vital nutrient in biology, and a significant component in seawater. The two stable isotopes of potassium (K) are mass 39 (ca. 93.3%) and 41 (ca. 6.7%), while radioactive ^{40}K (ca. 0.012%) decays to ^{40}Ar and ^{40}Ca. Potassium is also among the few remaining light elements with at least two stable isotopes whose variability in isotopic ratios due to mass-dependent fractionation in terrestrial systems has not been well characterized. This has been due, in part, to the difficulty of making high-precision analyses[3-7]. Measurements of ^{41}K/^{39}K by Humayun and Clayton[6, 8] identified fractionation in lunar soils and some meteorites but notably did not identify any samples resolvable from their terrestrial average with the precision attainable by ion microprobe (0.5‰, 2σ). Thermal Ionization Mass Spectrometry (TIMS) measurements are hindered by variable fractionation during individual analyses and the fact that K has too few isotopes to apply an internal spike method for instrumental mass fractionation corrections[5, 9].

High-precision measurements of stable K isotopes by multi-collector inductively coupled plasma mass spectrometry (MC-ICP-MS) present a number of analytical challenges because the Ar carrier gas produces hydrides with isobaric interferences on both ^{39}K (^{38}ArH$^+$) and ^{41}K (^{40}ArH$^+$). Recent studies by Li et al.[1] and Wang and Jacobsen[2] using MC-ICP-MS instruments with collision cells (GV Isoprobe P) have been able to reduce isobaric interferences on both ^{39}K and ^{41}K and achieved external precision on measured ^{41}K/^{39}K ratios of ~0.1-0.2‰ on natural samples. They demonstrated, as we have previously[10-12], a difference in the δ^{41}K values of seawater and silicate Earth. In this study, we present new high-precision

View Article Online
DOI: 10.1039/C7JA00257B

measurements of $\delta^{41}K$ values (defined as $(^{41}K/^{39}K_{sample} - {}^{41}K/^{39}K_{standard})/{}^{41}K/^{39}K_{standard}$ x 1000, relative to NIST KCl elemental SRM 999b) on a large number (n = 81) of natural samples using a MC-ICP-MS (Thermo Scientific NEPTUNE *Plus*) instrument run in high-resolution mode and cold plasma conditions to reduce isobaric interferences[13, 14].

Our suite of samples is broad and was selected from igneous, metamorphic, and siliciclastic whole rocks and minerals (n = 57), evaporite minerals and fertilizers (n = 9), hydrothermal minerals (n = 8) and plant and animal tissues (n = 7). The breadth of our sample suite is designed to provide both a survey of $^{41}K/^{39}K$ in geological and biological systems and to highlight particular areas in the bio and geosciences where there appears to be large and systematic variability in $^{41}K/^{39}K$ ratios that merits further investigation. Our results 1) confirm the observation by Wang and Jacobsen[2] and Morgan et al.[10, 15] that the $\delta^{41}K$ value of seawater is ~0.54‰ heavier than bulk silicate Earth (calculated from the mean of several whole-rock igneous samples, as noted with "**" in Appendix Table A.1); 2) show that there is significant variability in $\delta^{41}K$ values within granitic pegmatite systems; 3) provide further evidence of K isotope variability in biological systems, and 4) have implications for K-based geochronology and the atomic weight of K. This study demonstrates analytically resolvable natural variations in $^{41}K/^{39}K$ ratios in a wide range of geological and biological systems and suggests that future studies using high-precision K isotopic analyses can yield important new insights into the cycling of potassium on Earth's surface and in its interior.

2. Methods

2.1 Sample Set

View Article Online
DOI: 10.1039/C7JA00257B

Whole-rock and mineral samples were sourced largely from the collections of the Hunterian Museum of the University of Glasgow, whereas silicate standards were purchased from the U.S. Geological Survey (USGS; AGV-2, BCR-2, BHVO-2, GSP-2, QLO-1, SBC-1, SDC-1, SGR-1, and W-2a). Biological samples were sourced from grocery stores, butchers, and fishmongers in Scotland. Samples have been categorized into several groups: biological, evaporite, igneous (with a pegmatite subgroup), metamorphic, sedimentary, and hydrothermal samples. Detailed information for all samples (including museum collection numbers where applicable) for these samples is provided in Appendix Table A.1.

2.2 Sample dissolution

Mineral and rock samples were dissolved at either the Scottish Universities Environmental Research Centre (SUERC) or Princeton University. At SUERC, dissolution was achieved using trace-metal clean HF (40%) and HNO_3 (70%) in PFA Teflon vials kept overnight on a hotplate, followed by HNO_3 (70%) and HCl (36%) treatments under the same protocol. Plant and animal tissues were treated with aqua regia (3 parts HCl : 1 part HNO_3), followed by multiple treatments with H_2O_2. Evaporite samples were dissolved in HNO_3 (70%) and HCl (36%), also at SUERC. At Princeton, A CEM MARS 6 system was used to digest all USGS whole-rock standards following a four-step process: 1) Approximately 20 mg of sample powder were weighed into a 100 mL PFA Teflon digestion vessel and mixed with trace-metal clean HF (40%, 5 mL) and HNO_3 (70%, 5 mL). Sample was dissolved for 30 minutes at high temperature and pressure (200□, 400 psi) in the MARS 6 system. 2) Solution was dried in a vacuum for ca. 40 minutes in a CEM Teflon evaporation system. 3) Trace-metal clean HCl (36%, 3 mL) was added to the vessel, which was digested for 30 minutes at 200□ and 400 psi. 4) Dissolved samples were transferred into 15 mL PFA Teflon vials, dried overnight on a hotplate, and re-dissolved in 0.2% or 2% HNO_3 for potassium separation and mass spectrometry. USGS standards were tested for complete digestion by comparisons of their major element compositions against published values (Appendix Table A.2). Major element data for these standards were measured on a Thermo Finnigan Element-2 and ICAP-Q

View Article Online
DOI: 10.1039/C7JA00257B

inductively coupled plasma mass spectrometer (ICP-MS) using a set of matrix-matched in-house standards spanning the sample range[16]. The external reproducibility of this method for the elements used in this study is estimated at ± 10% (2σ).

2.3 Ion Exchange Chromatography

Separation of K from other matrix cations (e.g. Ca, Mg, Na) was accomplished using an automated Dionex ICS-5000+ ion chromatography system, which permits simultaneous determination of cation yield and the quality of the chromatographic separation (Figure 1)[17-19]. All samples were fully dissolved in 0.2% HNO_3 prior to loading onto a Dionex CS-16 cation exchange column and K was purified from the rest of the sample matrix using methanesulfonic acid (MSA) as the eluent. Yield for each sample was calculated from the chromatogram of conductivity generated for each sample (Figure 1) and samples with <99% yield were excluded from isotope analysis. To ensure purity, many of the separated K solutions were analyzed on a Thermo Scientific Element 2 inductively coupled plasma mass spectrometer (ICP-MS). Quantitative recovery of K was also tested by repeated separations of the NIST SRM 999b KCl standard on the Dionex system. Measurements of purified SRM 999b against SRM 999b straight from stock yielded values indistinguishable from 0‰ at our 2σ uncertainty. The MSA is removed from the sample by the suppressor in the Dionex system, and is not expected to contaminate the K fraction. Additional tests, which speak to the accuracy, precision, and reproducibility of this method, are described in detail in Section 2.4.1. Blanks from the column chromatography were small (average of 7 ± 12 mV (2σ) ^{39}K, and range from 0.06 to 1.06% of sample and standard ^{39}K signals, (n=79) compared with sample and standard sizes (typically 2-4 V ^{39}K).

2.4 Mass Spectrometry

View Article Online
DOI: 10.1039/C7JA00257B

High-precision measurements of stable K isotopes by multi-collector inductively coupled plasma mass spectrometry (MC-ICP-MS) present a number of analytical challenges because the Ar carrier gas produces hydrides with isobaric interferences on both ^{39}K ($^{38}ArH^{+}$) and ^{41}K ($^{40}ArH^{+}$). In standard hot plasma conditions, the intense ^{40}Ar beam could also pose problems in terms of ion scattering within the collector housing. Here, we use cold plasma conditions (500-600W[13, 14]) to preferentially suppress Ar ionization and reduce the production of $^{40}ArH^{+}$, in combination with high mass-resolution (M/ΔM ca. 10,000, measured at 5% and 95% relative peak height) on the Princeton University Thermo Scientific NEPTUNE *Plus* MC-ICP-MS instrument. Cold plasma reduces the production of $^{40}ArH^{+}$ to <30 mV and allows for the measurement of $^{41}K/^{39}K$ isotopic ratios on small (0.002 – 0.003 atomic mass units (amu)), flat, hydride interference-free peak shoulders (Figure 2).

Plasma and focusing parameters were tuned to optimize sensitivity, stability, size of the $^{40}ArH^{+}$ interference, and peak shape. The magnet on the NEPTUNE Plus is sufficiently stable so that the peak shoulder typically remains centered throughout an overnight set of analyses and often over the course of several days, even without performing peak-centering routines. Gas flow rates were run at relatively high levels (ca. 18 L/min, 1-1.2 L/min, and 1.1-1.6 L/min, for the cooling, auxiliary, and sample gas flows, respectively). These and other parameters are noted in Table 1. However, it should be noted that optimal gas flow and tuning varied considerably between sessions. The torch "Z" position is important in obtaining stability and is often pulled "back" from more typical run positions; this suppresses $^{40}ArH^{+}$ formation. Most samples and experiments were run using a quartz spray chamber; however, the APEX nebulizer was used for some duplicate measurements of USGS standards and the fractionation experiment. The APEX system appeared to introduce a bias in measurements that was corrected by normalization to BSW; following normalization of both APEX and quartz spray chamber data in this way, reproducibility between these two inlet systems is comparable to that from a single system. The

View Article Online
DOI: 10.1039/C7JA00257B

mean $\delta^{41}K$ values for all BSW runs (normalized only by sample-standard bracketing) are -0.071‰ for runs using the spray chamber, and -0.078‰ for runs using the APEX.

An analytical session begins by switching the instrument on to full radio frequency (RF) power (1200 W), then stepping down (steps of ca. 100 W) the RF to ca. 600 W. A standard is then aspirated for 20-30 minutes prior to tuning. Following tuning for sensitivity and peak shoulder flatness, several standard-standard bracketing measurements are made to ensure stability and accuracy.

The $^{38}ArH^+$ beam was determined to be negligible based on the $^{40}ArH^+$ signal intensity of ca. 20 mV and the atmospheric $^{38}Ar/^{40}Ar$ value of $6.3x10^{-4}$, [20]. Given the typical ^{39}K signal size of 2-4 V (for 2 ppm K solutions), this would create a potential bias of ca. 3.5×10^{-4}%. Even allowing for somewhat non-atmospheric Ar isotopic compositions, this bias is negligible. Although the ^{40}Ar beam is also significantly reduced (to ca. 30 mV; it is collected to monitor the stability of plasma conditions), the NEPTUNE Plus does not have the mass resolution to separate this beam from ^{40}K and thus ^{40}K measurements by ICP-MS remain elusive. Drift in instrument mass bias was taken into account using standard-sample-standard bracketing and each sample was measured two to three times during a single analytical session. Most analyses consisted of 1 block of 25 cycles with integration times of 8.389 seconds; some analyses consisted of 1 block of 80 cycles with integration times of 2.097 seconds. Sample and standard concentrations were matched within ca. 10%, as large imbalances may lead to artifacts in measured isotopic ratios[21, 22]. Finally, acid concentrations can also significantly affect measured $\delta^{41}K$; samples and standards were all diluted using the same batch of 2% HNO_3 to maintain strict consistency of acid concentrations.

We have tested the sensitivity of our analytical method to non-isobaric matrix effects. We also show, through mixing experiments of samples with distinct $\delta^{41}K$ values and deliberate mass-dependent

View Article Online
DOI: 10.1039/C7JA00257B

fractionation of K during ion-exchange chromatography, that our measured $\delta^{41}K$ values reflect real mass-dependent K isotope variability with an uncertainty of ca. 0.17‰ (2σ). These uncertainties, based on full sample replicates of modern seawater, are >15 times smaller than the range of $\delta^{41}K$ values in geological and biological samples measured in this study.

2.4.1 Tests for precision, reproducibility, matrix- and mass-dependence

The new analytical methods presented here require verification of several aspects of the procedures. We performed several tests to support the accuracy of $\delta^{41}K$ values presented herein: 1) characterization of the precision and reproducibility, both analytical and long-term, 2) the effects of sample matrix impurities on measured $\delta^{41}K$ values, and 3) the ability of the method to identify mass-dependent isotopic fractionation of K, including an experiment where standards are intentionally fractionated during K separation, and a mixing experiment involving the volumetric mixing of samples with different $\delta^{41}K$ values in a range of proportions.

2.4.1.1 Precision and reproducibility

Most standard and sample analyses yielded $^{41}K/^{39}K$ values with internal errors of ca. 0.01‰ to 0.03‰ (single measurement, ca. 200 seconds). Within-run precisions, resulting from the analysis of two to three standard-sample-standard bracketing measurements, range from <0.01‰ to ca. 0.29‰ (2σ) depending on plasma stability during the run.

The long-term external reproducibility of our method is estimated from replicate analyses of a set of international and in-house standards including seawater, SRM-70b (K-feldspar), and SRM-999b (KCl), at least two of which are chromatographically separated and isotopically analyzed in replicate alongside

View Article Online
DOI: 10.1039/C7JA00257B

each set of samples. Due to small (~0.1‰) systematic drift between analytical sessions, and particularly when using the APEX nebulizer, we find that normalizing values from each analytical session to the $\delta^{41}K$ value of seawater run during that same analytical session results in improved external reproducibility compared to $\delta^{41}K$ values of samples normalized only to the bracketing standard. The BSW standard that we normalize to has undergone K separation in the same batch as samples for that run, because small differences in the composition of the sample/standard matrix can lead to differences in instrumental mass bias and less precise/accurate results. We suspect, though cannot confirm, that these small matrix effects are associated with organic contaminants from the resin. This is a method that is also used in Ca measurements in our lab[23]. For N = 54 pairs of seawater measurements ($\delta^{41}K$ = 0‰), our external reproducibility (2σ) is 0.17‰ (Appendix Table A.3). For SRM-70b, N = 33 individual analyses, representing 11 separate digestions, yielded an average $\delta^{41}K$ value of -0.68 ± 0.17‰ (2σ) while for SRM-999b, N = 55 individual analyses yielded an average $\delta^{41}K$ value of -0.03 ± 0.17‰ (2σ). Based on all these standard measurements, we argue that ± 0.17‰ (2σ) is a reasonable estimate of the long-term reproducibility of our method. This is the uncertainty quoted for samples that are digested, chromatographically separated, and isotopically measured a single time. For samples that undergo multiple chromatographic separations and isotopic analyses, we also report the standard error of the mean (SE).

In this study, we use modern seawater as our isotopic reference scale (i.e. $\delta^{41}K$ of modern seawater = 0‰). We find that modern seawater is an ideal isotopic standard for major elements as it requires some (but not excessive) chromatographic purification, is readily accessible, likely to be isotopically uniform (to within ~0.1‰), and is more easily adopted by laboratories that pursue potassium isotope studies in materials other than silicate rocks. We note that our standardization is different than that used by Wang and Jacobsen[2], who chose to normalize $\delta^{41}K$ values to bulk silicate Earth.

View Article Online
DOI: 10.1039/C7JA00257B

2.4.1.2 Matrix effects

The influence of non-spectral matrix effects on measured isotopic ratios can be particularly problematic in cold plasma conditions[21, 24, 25]. To test the sensitivity of our method to the sample matrix remaining after single pass ion-exchange chromatography, we used two pure K standards spiked with matrix cations, one high in Mg and the other in Ca (the two most likely major contributors based on ion exchange chromatograms) but also containing smaller amounts of several other elements (Appendix Table A.4). These solutions were mixed with pure K standards and each mixture measured for δ^{41}K values (note that the Mg solution was made using a different source of K, and values are corrected in Appendix Table A.4 to the SRM 999b standard). The Mg-dominated solution was run in four different contaminant:K ratios, while the Ca-dominated solution was run in two. Also shown on Figure 3 and Appendix Table A.4 are several example measurements of impurities (as measured on the Element 2) in K separates for SRM 999b and BSW (Bermuda Seawater), both of which are expected to yield δ^{41}K values of ca. 0‰. Note that impurities for these (as well as impurities measured in the K separate for a whole-rock silicate sample, which is not expected to yield δ^{41}K values of 0‰) are all significantly lower than the point at which matrix appears to affect δ^{41}K values (ca. 20 to 30% impurities relative to K). These results suggest that the level and variability in sample matrix (including Ca and Mg, as well as Fe and other elements shown in Table A.4. from our procedure does not bias measured δ^{41}K values within our analytical uncertainties.

2.4.1.3 Accuracy and mass-dependent fractionation of K isotopes

To empirically test the accuracy of our method and our ability to identify mass-dependent variations in ^{41}K/^{39}K ratios, we deliberately fractionated K isotopes during ion chromatography by splitting the K peak for SRM 999b in three different parts (first, middle, and last; Figure 4). Each split was analyzed for their δ^{41}K values, which showed a negative correlation with peak elution time. The first, middle and last K cuts

View Article Online
DOI: 10.1039/C7JA00257B

varied systematically, having $\delta^{41}K$ values of 0.83 ± 0.16‰, -0.32 ± 0.09‰ and -0.45 ± 0.10‰, respectively. The weighted average of all 3 cuts for 4 different realizations of the experiment yielded a $\delta^{41}K$ value of -0.03 ± 0.10‰ (2σ), indistinguishable from the expected value of 0‰. An analogous experiment measuring Ca isotope ratios ($^{44}Ca/^{42}Ca$, $^{44}Ca/^{43}Ca$, and $^{43}Ca/^{42}Ca$) yielded qualitatively similar results, with peak cuts that were progressively depleted in the heavier ^{44}Ca isotope. For the Ca experiment, the first, middle and last peak cuts yielded $\delta^{44}Ca/^{42}Ca$ values of 4.05‰, -0.33‰, and -3.23‰, respectively. In this case, fractionation during column chromatography can be shown to be mass-dependent in three-isotope plots, as the measured isotope values lay along mass-dependent lines with a slope of ca. 0.5, consistent with theoretical predictions of mass-dependent fractionation[26]. It should be noted that this experiment was run using the APEX nebulizer, and values were normalized to seawater. By comparison, we conclude that the variability in $^{41}K/^{39}K$ ratios is also due to mass-dependent fractionation and note that the larger isotopic fractionation observed for Ca compared to K (for a similar mass difference) during ion chromatography is consistent with the greater affinity for Ca on the column resin.

The standard addition method[27] is used as an additional test for accuracy. Samples of markedly different $\delta^{41}K$ values and major element compositions—an evaporite (hanksite) with $\delta^{41}K$ = +0.45 ± 0.10‰ and a silicate (K-feldspar) with $\delta^{41}K$= -0.64 ± 0.02‰—were mixed in known volumetric proportions of K (25/75; 50/50; 75/25) prior to ion chromatography and isotopic analyses. Measured $\delta^{41}K$ values of these mixtures fall within analytical uncertainty of the expected 1:1 line (Figure 5) between the independently measured sample end-members.

3. Results

View Article Online
DOI: 10.1039/C7JA00257B

A summary of the measured $\delta^{41}K$ values for all n = 85 geological and biological samples and relevant supplemental data are given in Appendix Table A.1 and shown in Figure 6. The total variability observed in all samples is from -1.36‰ (N=2) in a lepidolite from the Glenbuchat pegmatite to 1.21‰ (N=5) in a kaliophilite from the Alban Hills, Italy. Silicate bulk rocks and minerals occupy the lower end of this range, and the average of n = 81 samples of bulk rock and mineral separates is -0.6 ± 0.58‰ (2σ). At the heavy end of the range is seawater, K-evaporite minerals (average $\delta^{41}K$ = +0.07 ± 0.69‰; 2σ, n =7), and two fertilizers (0.12‰ and 0.03‰). Our results also include samples also analyzed by Li et al.[1] (BCR-1, AGV-2, GSP-2, BCR-2, and BHVO-2), and Wang and Jacobsen[2] (BCR-2 and BHVO-2—although the latter used BHVO-1). Overall, there is excellent agreement between the analytical techniques, with all samples agreeing within quoted uncertainties.

3.1 Igneous and metamorphic whole rocks

Measured $\delta^{41}K$ values for eight igneous whole rocks (six of which are USGS rock standards) with compositions ranging from basalt to andesite to felsic glass, range from -0.48‰ to -0.58‰. The average of the eight whole rock samples is -0.54 ± 0.06‰, 2σ, which we define as our bulk silicate Earth (BSE) value. These are indicated in Figure 6 and Table A.1 with '**'. A carbonatite was also measured, with a value of -0.43 ± 0.13, 2σ.

Measured $\delta^{41}K$ values of three metamorphic whole rocks—a mica schist (USGS SDC-1) and a pseudotachylite vein/host rock pair in a tonalitic gneiss—range from -0.50 to -0.66‰, with an average of -0.56 ± 0.16‰, 2σ. Two impact melt rocks, from the Clearwater West and Rochechouart impacts, were also measured and yielded relatively light values of -0.90 and -0.71‰, respectively.

3.2 Igneous and metamorphic minerals

View Article Online
DOI: 10.1039/C7JA00257B

Measured $\delta^{41}K$ values from 19 of 20 samples of K-bearing igneous silicate minerals including orthoclase, anorthoclase, sanidine, hornblende, biotite, and phlogopite from a wide range of ages (Archean to Pleistocene) and locations average -0.50 ± 0.36‰ 2σ. The total range in $\delta^{41}K$ values is -0.01‰ to -0.77‰, but 15 of the 19 samples fall within 2σ (± 0.17‰) of the average of igneous whole rocks (-0.54‰). There is also no statistical difference between the $\delta^{41}K$ values of the different minerals—$\delta^{41}K$ of biotite = -0.63 ± 0.20‰ (2σ, N = 7), $\delta^{41}K$ of sanidine = -0.48 ± 0.06‰ (2σ, N = 4), and $\delta^{41}K$ of phlogopite = -0.50 ± 0.10‰ (2σ, N = 3). The one notable exception to this isotopic homogeneity are samples of nepheline and biotite from the Alban Hills, an ultrapotassic volcanic district emplaced along the Tyrrhenian margin of Italy during the Pleistocene[28, 29]. Although a sample of kalsilite from the same volcanic province has a measured $\delta^{41}K$ value of -0.51‰, the nepheline and biotite are significantly enriched in ^{41}K, at -0.01 and -0.18‰, respectively. The most significant outlier of all igneous samples measured here is a kaliophilite from the Alban Hills, with a $\delta^{41}K$ of +1.21 ± 0.26‰ (2σ, n = 5).

Measured $\delta^{41}K$ values of four samples of metamorphic minerals—two phengites, a neptunite, and a muscovite—are also somewhat enriched in ^{41}K compared to igneous whole rocks and minerals. Measured $\delta^{41}K$ values for these samples range from -0.21‰ (neptunite) to -0.45‰ (phengite), averaging -0.30 ± 0.20‰ (2σ, N = 4).

3.3 Pegmatites

In contrast to the relatively homogeneous $\delta^{41}K$ values observed in igneous and metamorphic whole rocks and minerals, a >1‰ range in $\delta^{41}K$ values—from -1.36 to -0.11‰—is observed in 17 minerals taken from a suite of igneous and metamorphic pegmatites. Measured minerals include K-feldspars (-0.32 to -1.19‰, n = 10), micas (-0.11 to -1.36‰, n = 7), and a sample of astrophyllite ($\delta^{41}K$ = -0.71‰). The

View Article Online
DOI: 10.1039/C7JA00257B

largest range in measured $\delta^{41}K$ values is observed between samples from different sites but also from different minerals within the same site. For example, K-feldspar, two muscovites, and lepidolite from within a single lithium pegmatite from Glenbuchat, Scotland, have measured $\delta^{41}K$ values of -0.65‰, -0.79‰, -1.31‰, and -1.36‰, respectively. Generally, the $\delta^{41}K$ values of the samples from pegmatites are depleted in ^{41}K ($\delta^{41}K = -0.78 \pm 0.76$‰, 2σ, n = 17) compared to bulk igneous whole rocks and mineral separates, though the range in $\delta^{41}K$ values observed in pegmatites includes samples that are also significantly enriched in ^{41}K compared to igneous whole rocks and minerals.

3.4 Sedimentary whole rocks

We analyzed two sedimentary whole-rock standards from the USGS (SGR-1b and SBC-1) that are measurably distinct in environment and geochemical composition. Sample SBC-1 is a marine shale from the Glenshaw Formation (Westmoreland County, PA) and SGR-1b is sourced from the Mahogany zone of the Green River Formation (Piceance Creek Basin, CO), a sequence with kerogenous dolomicrite shales deposited in a saline lacustrine environment[30]. Sample SBC-1 is within error of our bulk silicate Earth value with an average $\delta^{41}K$ value of -0.61 ± 0.12‰ (2σ, N = 5). In contrast, SGR-1b is enriched in ^{41}K compared to BSE and has an average $\delta^{41}K$ value of -0.25‰ ± 0.08‰ (2σ, N = 4).

3.5 Hydrothermal minerals

We analyzed eight samples from continental hydrothermal systems that include philipsite, apophyllites, adularia, jarosite, and alunite. Measured $\delta^{41}K$ values from these samples exhibit a relatively narrow range (average $\delta^{41}K = -0.57 \pm 0.23$‰; 2σ) and are indistinguishable from bulk silicate Earth.

3.6 Evaporites and industrial fertilizer

View Article Online
DOI: 10.1039/C7JA00257B

Measured $\delta^{41}K$ values of six marine and one lacustrine K-evaporites (sylvite, polyhalite, carnallite, kainite, and hanksite) range from -0.24‰ to +0.64‰. The average $\delta^{41}K$ value for all seven evaporites is 0.07 ± 0.68‰, 2σ. Two commercial NPK (nitrogen, phosphorus, potassium) fertilizers have measured $\delta^{41}K$ values of 0.12‰ and 0.03‰, indistinguishable from modern seawater and some K-evaporite minerals.

3.7 Biological samples

Biological samples include banana, potato, beef, lamb, scallop, prawn, and haddock. Measured $\delta^{41}K$ values for these samples vary between -0.88 ± 0.03‰, 2σ (lamb muscle) and +0.36 ± 0.04‰, 2σ (scallop adductor muscle). In general, organic matter from terrestrial mammals is isotopically lighter than plant material and marine organisms.

4. Discussion

Our results indicate that there are natural variations in the $^{41}K/^{39}K$ ratio of potassium in geological and biological samples that can be resolved at the ca. 0.1-0.2‰ level by MC-ICP-MS under cold plasma conditions. The total range in measured $\delta^{41}K$ values for N = 81 natural samples is 2.57‰, or >15x our estimated 2σ external reproducibility based on a large number (N=196) of replicate analyses of standards with very different matrices (seawater to silicates). The diverse set of samples analyzed provides an imperfect but tantalizing glimpse at variability of $^{41}K/^{39}K$ ratios in natural systems and suggests that this and future studies of K isotopes will make fundamental contributions to our understanding of the cycling of K in geological and biological systems. Measured $\delta^{41}K$ values from our diverse sample suite suggest the following:

View Article Online
DOI: 10.1039/C7JA00257B

1) The $\delta^{41}K$ values of whole rocks and minerals are relatively homogeneous in most igneous and metamorphic systems, in agreement with Li et al.[1] and Wang and Jacobsen[2], with the notable exception of pegmatites which show large variability in measured $\delta^{41}K$ values that range from -0.28 to -1.36‰, values that are both above and below the $\delta^{41}K$ value of bulk silicate Earth (-0.54‰).

2) The $\delta^{41}K$ value of seawater is ~0.6‰ enriched in ^{41}K compared to bulk silicate Earth, again in agreement with Wang and Jacobsen[2]. This offset could be a result of K isotope fractionation during secondary clay formation associated with (a) continental silicate weathering, (b) alteration of oceanic crust, and/or (c) diagenesis of marine sediments[31, 32].

3) The $\delta^{41}K$ values of biological samples range over 1.24‰, from -0.88 to +0.36‰. Terrestrial animals tend to be closer to bulk silicate Earth, while marine animals are closer to seawater.

4) The bias in $\delta^{41}K$ between BSE and the KCl standard previously measured for K atomic weight determinations indicates a need to reassess the atomic weight of K.

5) The difference in $\delta^{41}K$ between most silicate samples and KCl standards SRM 999b and 985 indicates a potential bias in $^{40}Ar/^{39}Ar$ ages of ca. 0.4‰.

Although the broad set of samples analyzed during this study cannot provide conclusive evidence for any particular mechanisms for K isotope fractionation in nature, the sample suite does have a common thread in that in many cases variability in measured $^{41}K/^{39}K$ ratios may be able to be explained by fractionation during diffusion. Diffusive fractionation of K isotopes has been shown to occur in both silicate melts[33, 34] and water[35] in the laboratory, and many of the samples included in this study come from systems where mass transport by diffusion may be important.

4.1 Sources of potassium isotope variability in igneous and metamorphic systems

View Article Online
DOI: 10.1039/C7JA00257B

With the exception of pegmatites and a few samples from continental arc and subduction-related settings, we observe little K isotopic variability in high-temperature igneous and metamorphic systems. Most igneous whole rock and mineral separates (25 of 29) have an average $\delta^{41}K$ value of -0.54 ± 0.19‰ (2σ) compared to modern seawater ($\delta^{41}K$ = 0‰), an uncertainty that is only slightly greater than the external reproducibility (2σ) of our analytical method (± 0.17‰). Our results also show excellent agreement with the recent study of Wang and Jacobsen[2] for both individual samples and our average for bulk silicate Earth. Our data set does not provide any strong evidence for inter-mineral fractionation—for example, biotite, sanidine and hornblende from the Fish Canyon Tuff all have indistinguishable $\delta^{41}K$ values (-0.50‰, -0.51‰, -0.44‰; Appendix Table A.1). Finally, similar $\delta^{41}K$ values are observed in both mafic and felsic whole rocks and minerals, suggesting that K isotope effects associated with magmatic differentiation are also small, similar to what is observed for Li [36], Mg [37], and Fe [38].

Exceptions to the K isotope homogeneity in igneous and metamorphic rocks and minerals include samples from the Alban Hills ultrapotassic volcanic province[28, 29] and metamorphic minerals in serpentinites and glaucophane schists of the Franciscan Complex[39]. In both cases, samples tend to be enriched in ^{41}K compared to average igneous whole rocks, averaging -0.23‰ (range of -0.50‰ to -0.01‰). One intriguing possibility is that the K in these systems has a significant source component from subducted oceanic crust and/or sediments that are enriched in ^{41}K, as the mass balance of K in the crust requires that much of the K taken down the trench as sedimentary drape or altered oceanic crust be returned to the crust through dewatering and partial melting of the subducting slab[40].

Additionally, measured $\delta^{41}K$ values in pegmatites vary more than most igneous and metamorphic whole rocks and minerals. Pegmatite phases vary by >1‰, from -0.11‰ to -1.36‰. These assemblages, generally interpreted as reflecting late-stage crystallization in systems where there is often a significant fluid component, are characterized by measured $\delta^{41}K$ values that are both enriched and depleted relative

View Article Online
DOI: 10.1039/C7JA00257B

to bulk silicate Earth. This variability can be observed on an outcrop scale and in one case, the Glenbuchat pegmatite is observed to correlate with independent petrographic and geochemical observations of the timing of crystallization. This zoned lithium pegmatite of probable Caledonian age in NE Scotland[41] was sampled (A, B, C) for both early and late assemblages based on petrographic relationships in both thin sections and outcrop. The $\delta^{41}K$ values of these minerals range from -0.65‰ and -0.79‰ in early K-feldspar and muscovite (A) to -1.31‰ and -1.36‰ in late-stage muscovite (B) and lepidolite (C), respectively, one of the last phases to crystallize in the central region of the pegmatite (Figure 7; petrographic and field relations by J. Faithfull). This interpretation—lower $\delta^{41}K$ values in later crystallizing assemblages—is supported by covariation between $\delta^{41}K$ values and measured Rb/K ratios of the muscovite samples (A and B). One possible explanation is again variations in the $\delta^{41}K$ value of the source, though in this case the $\delta^{41}K$ value of the source needs to be significantly depleted in ^{41}K compared to bulk silicate Earth. Another intriguing but not mutually exclusive possibility—K isotope fractionation due to chemical or thermal diffusion (Soret effect)—is suggested from previous studies in pegmatites utilizing Li isotopes and experimental observations[42]. In order to explain the observed decline in measured $\delta^{41}K$ values in the interior, later-crystallizing minerals by K isotope effects associated with chemical diffusion, one must invoke mineral growth with an increase in either the diffusive path-length or the K concentration gradient within the diffusive boundary layer as crystallization progresses. Along the same lines, thermal diffusion (Soret effects) may also contribute to the decline in $\delta^{41}K$ values in the later crystallizing phases in the interior of the pegmatite if there is a large temperature gradient (declining outward) into the surrounding country rock. In this case, the light K isotope (^{39}K) will be preferentially enriched in the warmer end of the thermal gradient, leading to low $\delta^{41}K$ values in the late-crystallizing phases in the interior. Other processes may be significant. Five subsamples drilled from M11650, a single crystal of amazonite feldspar, show a significant range of $\delta^{41}K$ values (Appendix Table A1). This crystal formed in a drusy cavity (i.e. at a silicate/hydrous-halide melt interface), suggesting the possibility of a link between melt unmixing and K isotope fractionation, perhaps aided by differences in

View Article Online
DOI: 10.1039/C7JA00257B

coordination/complexing between silicate and hydrous-halide melts. Although all of these explanations of our data are preliminary, the observation that there is large and systematic variability in mineral $\delta^{41}K$ values in pegmatites and some other igneous systems suggests that $\delta^{41}K$ values will be a useful new tool, in particular when paired with other major/minor metal isotopes (e.g. $\delta^{7}Li$, $\delta^{26}Mg$, $\delta^{56}Fe$), to interrogate magmatic processes and petrogenesis in these systems.

4.2 Sources of potassium isotope variability in low-temperature systems

Measured $\delta^{41}K$ values in marine K-evaporites vary by 0.9‰, but five of six samples are within ~0.2‰ of modern seawater, similar to the $\delta^{41}K$ values reported by Wang and Jacobsen[2]. The isotopically heavy Hartsalz sample is highly altered and may have experienced postdepositional alteration. Our results do not constrain K isotope fractionation in K-evaporites directly as all of our samples are ancient (Silurian to Permian). However, these measurements generally suggest that fractionation of K isotopes during the precipitation of marine K-evaporites is not large and furthermore K-evaporites do not constitute a significant sink of K from seawater.

4.3 Sources of potassium isotope variability in biological systems

Potassium is also a critical component in biological systems. It is the most abundant cation in intracellular fluids of all eukaryotes and is involved in the maintenance of electroneutrality and osmotic equilibrium in plant and animal cells, an essential requirement for life[43]. Potassium cell uptake can happen via both active ("pumps") and passive (ion channels) mechanisms. Active K uptake is mediated by the membrane proteins Na^{+},K^{+}-ATPase (the "sodium-potassium pump") in animal cells, and H^{+}-ATPase (the "proton pump") in plant cells[44]. Pilot data presented here are from several soft tissue samples of mammals, plants, and marine organisms. The potassium isotope composition of these organisms likely reflects 1) the $\delta^{41}K$

View Article Online
DOI: 10.1039/C7JA00257B

composition of its K source and 2) any potential K isotope fractionation during K uptake. Although our biological dataset is admittedly limited in scope, it is clear that biological systems fractionate K isotopes.

Sources of potassium vary across biological samples in this study. In the case of plants (represented by banana and potato), K is sourced from the breakdown of K-rich minerals in soils and/or fertilizers. Given that the K isotope composition of K-rich minerals shows a range of >1‰, the $\delta^{41}K$ composition of mineral-sourced potassium available to plants is potentially variable though it is generally expected to have a $\delta^{41}K$ value close to bulk silicate Earth (-0.54‰). A complicating factor in determining the $\delta^{41}K$ of this K source is that weathering can be accompanied by secondary clay formation, which has been suggested to fractionate K isotopes in marine sediments[31, 32]. In contrast, the bioavailable K in cultures treated with fertilizers is likely homogenous (e.g. MaxiGrow and RAW, see Appendix Table A.1); fertilizers have a K isotope composition similar to that of seawater and are isotopically enriched compared to most silicate minerals. In addition to variable K sources, plants have also been observed to fractionate K isotopes during uptake, with preferential incorporation of ^{39}K[45, 46].

Terrestrial and marine animals have measurably different K isotope compositions, and the mammals in this study (beef, lamb) yield overall lower $\delta^{41}K$ values than the marine organisms (haddock, prawn, scallop). Although the diet of a lamb or cow is not likely to include potato or Honduran banana, the isotopically light character of these mammals (avg. $\delta^{41}K$ = -0.68‰) suggests that biological processes may fractionate K and, in this case, may possibly indicate trophic level effects[47]. In contrast to terrestrial mammals, seawater is the single most important source of potassium to marine organisms. Because the $\delta^{41}K$ value of seawater is almost certainly homogeneous at the 0.1‰-level (due to the long residence time of potassium in the ocean), the variability seen here in the measured K isotope composition of haddock, prawn and scallop most likely reflects isotope fractionation during biological K uptake. Given that the concentration of K in seawater is higher than in the plasma of most marine organisms[48], chemical

View Article Online
DOI: 10.1039/C7JA00257B

gradients lead to passive diffusion of K from seawater into these animals. Bourg et al.[35] have demonstrated via experiments and molecular dynamic simulations that aqueous K diffusion is accompanied by K isotope fractionation ranging between 0.9967 and 0.9984, that is, ^{39}K diffuses faster than ^{41}K in aqueous solutions. These fractionations are much larger than the lightest marine organism measured here (prawn, -0.36‰), suggesting that either 1) the magnitude of diffusive K fractionation is smaller across these biological membranes and/or 2) active K secretion through Na^+,K^+-ATPase pumps also fractionates K isotopes. If both passive and active K transport mechanisms are associated with fractionation favoring the light isotope (^{39}K), the range in $\delta^{41}K$ values of marine organisms observed here could reflect differences in K isotope fractionation associated with active or passive transport (or both).

4.4 Atomic weight calculations and relative isotopic abundances of K

Atomic weights are used by the scientific and technological communities for a wide range of physical constants and laws, as well as metrological, legal, and international standards[49, 50]. Current IUPAC (International Union of Pure and Applied Chemistry) values for the atomic weight and isotopic abundances of K[49] are largely based on a calibration of SRM 985 by Garner et al.[5], who also noted that 80 minerals analyzed by similar methods (TIMS) showed no major variations in $^{41}K/^{39}K$ but that the average of these was ca. 0.3‰ lighter than SRM 985 (a NIST isotopic SRM that is no longer available). Data for these 80 minerals were never published, and this difference was attributed to analytical issues. Subsequently, Humayun and Clayton[6] observed a difference of ca. 0.7‰ (in the same direction) between SRM 985 and their "terrestrial average." Despite this apparent isotopic difference between rocks and minerals and SRM 985, the current atomic weight and relative isotopic abundances of K[49] are largely based on values obtained by Garner et al.[5] for SRM 985. Our data indicate SRM 985 is 0.259 ± 0.069‰ (2σ) heavier than seawater, which is indistinguishable from NIST elemental K SRM 999b (-0.03 ± 0.17‰; Figure 2b, Figure 8).

View Article Online
DOI: 10.1039/C7JA00257B

Naumenko et al.[51] made high-precision measurements of ^{40}K in standard reference materials (SRM 918b and SRM 985) by TIMS. The most precise of their methods requires a normalizing value of known $^{41}K/^{39}K$; Naumenko et al.[51] assumed a value determined by Garner et al.[5] for both standards. Although this is a reasonable assumption for SRM 985, results herein indicate that $^{41}K/^{39}K$ values for standard reference materials (e.g. SRM 985 and SRM 999b) can vary by as much as ca. 0.30‰ (0.259 ± 0.069% for SRM 985 vs. BSW), and thus $^{41}K/^{39}K$ values should be measured directly prior to ^{40}K measurements by TIMS. The difference found here between SRM 985 and SRM 999b indicates that results of Naumenko et al.[51] may be biased by ca. 0.15‰.

Our data also indicate that our bulk silicate Earth (BSE) value (the average of several igneous whole-rock values) is in turn significantly isotopically lighter than BSW (Figures 6, 8), at -0.544 ± 0.061‰, 2σ. This BSE value is thus offset relative to SRM 985 by -0.803 ± 0.092‰ (2σ, calculated using analytical precision for both values) and can be used to calculate an "absolute" $^{41}K/^{39}K$ ratio for the BSE of 0.0721098 ± 0.000032, 2σ, as shown in Figure 8. Uncertainties here are slightly higher than those from Garner et al.[5] for SRM 985 as they incorporate the analytical uncertainties involved in determining $\delta^{41}K$ values for SRM 985 relative to the BSE (via SRM 999b and with all measurements normalized to BSW) in addition to the uncertainties from Garner et al.[5]. It should be noted that this offset of ca. 0.80‰ between SRM 985 and the BSE is indistinguishable from that observed by Humayun and Clayton[6]. Although preliminary, these data clearly show that the isotopic abundances for K should be revisited, for example, following the methods employed by Rudnick and Gao[52]. The geological variability identified herein indicates a need to fully assess the range of terrestrial variation for future compilations. Further, a rigorous assessment of isotopic abundances and the atomic weight of K should rely on ^{40}K measurements; if we assume the ^{40}K isotopic abundance to be the same as published in IUPAC[49], isotopic abundances for

View Article Online
DOI: 10.1039/C7JA00257B

^{39}K and ^{41}K become 0.932631 and 0.0672518, respectively. Similarly, the atomic weight for K becomes 39.0982 u, which is 0.0001 u lighter than (although within 2σ of) the current IUPAC value[49].

4.5 Effects on K-Ar and ^{40}Ar/^{39}Ar geochronology

Potassium isotopic abundances of silicates are also significant as K is the parent element for the K-Ar and ^{40}Ar/^{39}Ar geochronometers. These chronometers are widely applied over ka to Ga timescales to constrain timing in geology, paleontology, archaeology, planetary sciences, environmental sciences, and the calibration of geological timescales.

Notably, Naumenko et al.[51] motivate their study with the claim that the absolute abundance of ^{40}K (i.e., the terrestrial ^{40}K/K value) is a major source of uncertainty in K-Ar and ^{40}Ar/^{39}Ar geochronology. This misunderstanding is reiterated to some extent by Wang and Jacobsen[2]. In fact, the absolute value of ^{40}K/K does not affect calculated ages. Rather, biases are introduced from any variation between the ^{40}K/K values of material used for decay constant determination, those of mineral standards (i.e., neutron flux monitors), and those of samples of interest. This issue of differences is important because it is unclear what materials have previously been used in determinations of the ^{40}K decay constant[53-56], but given the differences found between NIST K standards and silicate mineral phases measured here (ca. 0.8‰ bias), it is likely that at least some variability exists. Potential relative age biases would be approximately half of the difference in δ^{41}K (thus ca. 0.4‰). Age modeling results show that calculating the age of Fish Canyon sanidine, using GA1550 as a neutron flux monitor, assuming each has ^{41}K/^{39}K as determined herein (Appendix Table A.1), and assuming decay constants were determined on KCl with ^{41}K/^{39}K equal to that of SRM 985, the calculated age of Fish Canyon sanidine is biased by 0.38‰. These differences represent a small but potentially important effect for ^{40}K-based geochronology, particularly as analytical precision

View Article Online
DOI: 10.1039/C7JA00257B

has approached 0.5‰[57] with the recent developments in next generation multi-collector noble gas mass spectrometers.

5. Conclusions

The development of new methodology for the measurement of $\delta^{41}K$ values using a Thermo Scientific NEPTUNE *Plus* MC-ICP-MS has allowed for the identification of variability in $\delta^{41}K$ in a range of systems. The approach taken here relies on high-purity K separations, and analysis in cold plasma, high-resolution mode on the NEPTUNE *Plus*. We find that the $\delta^{41}K$ value of bulk silicate Earth is -0.54‰ relative to modern seawater, in agreement with a recent study by Wang and Jacobsen[2], and attesting to the efficacy of our new analytical approach (cold plasma vs. collision cell).

We also provide a number of potential applications of K isotopes as a biogeochemical proxy: 1) we observe that K isotope fractionation in high-temperature igneous and metamorphic whole rocks and minerals is generally small, with the notable exception of pegmatites and possibly arc systems where there are large contributions of K from the subducted slab; 2) we find that fractionation of K isotopes may occur during both passive and active K exchange between seawater and marine organisms. In addition, the K isotope composition of muscle tissue from terrestrial mammals might also indicate trophic level effects in K isotope distribution, given its lighter K isotope composition compared to our plant samples; in both cases, additional studies are needed to determine what controls K cycling in biological systems; and 3) our data indicate a need to reassess the atomic weight of potassium and possibly to incorporate $\delta^{41}K$ measurements in very high-precision $^{40}Ar/^{39}Ar$ geochronology.

Conflicts of Interest

View Article Online
DOI: 10.1039/C7JA00257B

N.S.L. is employed by ThermoFisher Scientific, the company which manufactures the NEPTUNE *Plus* ICP-MS used and described herein. The authors have no other conflicts of interest to report.

Acknowledgements

We thank Tony Fallick, Tom Preston, Darren Mark, Justin Simon, Mike Tappa, Ryan Mills, Jason Newton, Blair Schoene, Brenhin Keller, Daniel Stolper, and Jim Watkins for helpful discussions and comments on drafts. The technical advice and support from Elaine Dunbar, Anne Kelly, Gillian MacKinnon, and Liz Lundstrom are greatly appreciated. We thank Darren Mark, Thijs van Soest, Bob Perkins, Paul Renne, and Dan Barfod for providing samples.

While at SUERC, LM was funded by a Marie Curie Intra-European Fellowship. Travel funds were provided by an Earthtime-EU Short Visit Grant. Laboratory work was supported by Princeton University.

Any use of trade, product, or firm names is for descriptive purposes only and does not imply endorsement by the U.S. Government.

Figure Captions

Figure 1. Ion chromatograph of a K separation run on the Thermo Scientific Dionex ICS5000+. Typical K collection window is shaded in gray, although the exact position varies due to variable sample matrices. Note complete separation of K peak from Na, Mg, and Ca peaks and quantitative K peak recovery.

Figure 2. Peak shoulder measurements made on masses 39 and 41. For mass 41, both the shoulder of ^{41}K and the combined peak of ^{41}K and $^{40}ArH^{+}$ are shown. Note that measurements are made on the peak shoulder for mass 41, but the relative fraction of atmospheric ^{38}Ar is sufficiently small that the $^{38}ArH^{+}$

View Article Online
DOI: 10.1039/C7JA00257B

interference on the ^{39}K peak would be negligibly small under typical run conditions; thus measurements are made near the center of the mass 39 peak.

Figure 3. Results from two separate matrix experiments, where standards were doped with varying amounts of impurities to determine at which point matrix will affect measured $\delta^{41}K$ values. Solutions with Mg as the major contaminant are shown as circles, and those with Ca as the major contaminant are shown as squares. Several example K separates, including seawater and a whole-rock silicate, are shown in triangles. Data are provided in Table A.3.

Figure 4. Results from fractionation experiments run on the Thermo Scientific Dionex ICS5000+. Four K and two Ca standards were run through system, and the peak of interest was collected in three separate cuts. Results from each K experiment are shown, along with the average of the two Ca experiments. For each experiment, the first cut yielded heavier $\delta^{41}K$ values, followed by progressively lighter middle and last cuts. Uncertainties represent within-run precision (2σ).

Figure 5. Results from mixing experiment between two samples, Hanksite and K-feldspar. $\delta^{41}K$ values for each are shown, along with $\delta^{41}K$ values for mass-based mixtures of K with varying relative amounts of each sample end-member. Uncertainties for individual analyses are shown at 0.15‰ (long-term 2σ). Shaded region encompasses the expected $\delta^{41}K$ of mixed solutions given the long-term reproducibility of our method.

Figure 6. $\delta^{41}K$ values for terrestrial samples and standards, relative to NIST SRM 999b. Data are provided in Table A.1. Uncertainties are estimated at the 2σ level and represent either within-run uncertainties (for samples with a single run) or precision between runs (for samples with multiple runs).

View Article Online
DOI: 10.1039/C7JA00257B

For reference, long-term reproducibility is indicated separately. **(a)** Pegmatite and other high-temperature terrestrial silicates. **(b)** Siliciclastic rocks, evaporites, hydrothermal, biological, and standard samples.

Figure 7. $\delta^{41}K$ values for phases from suite of pegmatite samples from Glenbuchat, Scotland, shown against Rb/K values, which may be considered a proxy for melt evolution. Within-run precisions (2σ) are shown in black; long-term reproducibility (2σ) is shown as larger white boxes. In order from low to high Rb/K, samples are: 1) k-feldspar from sample A, 2) muscovite from sample A, 3) muscovite from sample B, 4) lepidolite from sample C. See text section 4.1 and Table A.1 for sample descriptions.

Figure 8. $^{41}K/^{39}K$ values for SRM 985 (value and uncertainty from Garner et al. 1975), the recommended IUPAC value, SRM 999b, and the mean of selected samples analyzed here that are considered representative of crustal values. Uncertainties (all 2σ) for the latter two are represented in black for within-run precision (SRM 999b) and the variation in selected samples ('bulk Earth'), and in white including the absolute uncertainty in the $^{41}K/^{39}K$ value SRM 985 as determined by Garner et al.[5].

Table Captions

Table A.1. Summary of data for samples presented herein, as shown in Figure 6. $\delta^{41}K$ values and uncertainties are presented along with information for each sample. For samples separated >1 time, uncertainty is based on the standard deviation of multiple runs. For samples separated only once, uncertainty is provided based on the long-term reproducibility of seawater (0.17‰). All values are normalized to seawater analyzed during the same session.

Table A.2. Major element geochemistry for USGS standards with $\delta^{41}K$ values presented herein. Values agree with USGS values, indicating complete digestion of silicates with our methods. We assumed the reported USGS Al_2O_3 values to calculate the remaining oxide compositions from measured X/Al ratios.

View Article Online
DOI: 10.1039/C7JA00257B

Table A.3. $\delta^{41}K$ values for BSW samples collected over the course of the study. These data are used to calculate the long-term reproducibility value of 0.17‰. All values are normalized to the average of seawater measurements within that run.

Table A.4. Data from matrix experiments shown in Figure 4 and described in section 2.5.1.2. Major and total contaminant percentages are shown for each experiment, along with $\delta^{41}K$ values and the levels of other contaminants in each solution. Also shown are contaminant levels and $\delta^{41}K$ values for several K separates of samples and standards.

References

1. W. Li, B. L. Beard and S. Li, *Journal of Analytical Atomic Spectrometry*, 2016, **31**, 1023-1029.
2. K. Wang and S. B. Jacobsen, *Geochimica et Cosmochimica Acta*, 2016, **178**, 223-232.
3. A. K. Brewer, *Journal of Industrial and Engineering Chemistry*, 1938, **30**, 893-896.
4. A. K. Brewer and P. D. Kueck, *Physical Review*, 1934, **46**, 894-897.
5. E. L. Garner, T. J. Murphy, J. W. Gramlich, P. J. Paulsen and I. L. Barnes, *Journal of Research of the National Bureau of Standards*, 1975, **79**, 713-725.
6. M. Humayun and R. N. Clayton, *Geochimica et Cosmochimica Acta*, 1995, **59**, 2115-2130.
7. A. A. Verbeek and G. D. L. Schreiner, *Geochimica et Cosmochimica Acta*, 1967, **31**, 2125-&.
8. M. Humayun and R. N. Clayton, *Geochimica et Cosmochimica Acta*, 1995, **59**, 2131-2148.
9. D. Wielandt and M. Bizzarro, *Journal of Analytical Atomic Spectrometry*, 2011, **26**, 366-377.
10. L. Morgan, J. Higgins, B. Davidheiser-Kroll, N. Lloyd, J. Faithfull and R. Ellam, presented in part at the Goldschmidt Conference, Sacramento, 2014.
11. L. E. Morgan, M. Tappa, R. M. Ellam, D. F. Mark, N. S. Lloyd, J. A. Higgins and J. I. Simon, presented in part at the American Geophysical Union Fall Meeting, San Francisco, 2013.
12. L. E. Morgan, N. S. Lloyd, R. M. Ellam and J. I. Simon, presented in part at the American Geophysical Union Fall Meeting, San Francisco, 2012.
13. J. S. Becker and H. J. Dietze, *Journal of Analytical Atomic Spectrometry*, 1998, **13**, 1057-1063.
14. K. E. Murphy, S. E. Long, M. S. Rearick and O. S. Ertas, *Journal of Analytical Atomic Spectrometry*, 2002, **17**, 469-477.
15. L. Morgan, D. Santiago Ramos, N. Lloyd and J. Higgins, presented in part at the Goldschmidt Conference, Paris, 2017.
16. Y. Rosenthal, M. P. Field and R. M. Sherrell, *Analytical Chemistry*, 1999, **71**, 3248-3253.
17. C. L. Blättler, N. R. Miller and J. A. Higgins, *Earth and Planetary Science Letters*, 2015, **419**, 32-42.
18. M. S. Fantle and J. Higgins, *Geochimica et Cosmochimica Acta*, 2014, **142**, 458-481.
19. J. M. Husson, J. A. Higgins, A. C. Maloof and B. Schoene, *Geochimica et Cosmochimica Acta*, 2015, **160**, 243-266.

View Article Online
DOI: 10.1039/C7JA00257B

20. J.-Y. Lee, K. Marti, J. Severinghaus, K. Kawamura, H. Yoo and J. Kim, *Geochimica et Cosmochimica Acta*, 2006, **70**, 4507-4512.
21. F. Albarède and B. Beard, *Reviews in Mineralogy and Geochemistry*, 2004, **55**, 113-152.
22. M. E. Wieser, D. Buhl, C. Bouman and J. Schwieters, *Journal of Analytical Atomic Spectrometry*, 2004, **19**, 844-851.
23. C. L. Blättler and J. A. Higgins, *Geology*, 2014, **42**, 711-714.
24. C. J. Bryant, M. T. McCulloch and V. C. Bennett, *Journal of Analytical Atomic Spectrometry*, 2003, **18**, 734-737.
25. S. J. Jiang, R. S. Houk and M. A. Stevens, *Analytical Chemistry*, 1988, **60**, 1217-1221.
26. E. D. Young, A. Galy and H. Nagahara, *Geochimica et Cosmochimica Acta*, 2002, **66**, 1095-1104.
27. E. T. Tipper, P. Louvat, F. Capmas, A. Galy and J. Gaillardet, *Chemical Geology*, 2008, **257**, 65-75.
28. D. B. Karner and P. R. Renne, *Geological Society of America Bulletin*, 1998, **110**, 740-747.
29. F. Marra, C. Freda, P. Scarlato, J. Taddeucci, D. B. Karner, P. R. Renne, M. Gaeta, D. M. Palladino, R. Trigila and G. Cavarretta, *Bulletin of Volcanology*, 2003, **65**, 227-247.
30. R. Cole, 1985.
31. D. P. Santiago Ramos, L. E. Morgan, N. S. Lloyd and J. A. Higgins, *Geochimica et Cosmochimica Acta*, submitted.
32. D. Santiago Ramos and J. Higgins, presented in part at the Goldschmidt Conference, Paris, 2017.
33. G. Goel, L. Zhang, D. J. Lacks and J. A. Van Orman, *Geochimica et Cosmochimica Acta*, 2012, **93**, 205-213.
34. F. M. Richter, E. B. Watson, M. Chaussidon, R. Mendybaev, J. N. Christensen and L. Qiu, *Geochimica et Cosmochimica Acta*, 2014, **138**, 136-145.
35. I. C. Bourg, F. M. Richter, J. N. Christensen and G. Sposito, *Geochimica et Cosmochimica Acta*, 2010, **74**, 2249-2256.
36. P. B. Tomascak, F. Tera, R. T. Helz and R. J. Walker, *Geochimica et Cosmochimica Acta*, 1999, **63**, 907-910.
37. F.-Z. Teng, M. Wadhwa and R. T. Helz, *Earth and Planetary Science Letters*, 2007, **261**, 84-92.
38. F.-Z. Teng, N. Dauphas and R. T. Helz, *Science*, 2008, **320**, 1620-1622.
39. J. Wakabayashi, *International Geology Review*, 2015, **57**, 669-746.
40. F. Albarède, *Tectonophysics*, 1998, **296**, 1-14.
41. B. Jackson, *Journal of Gemmology*, 1982, **18**, 121-125.
42. F. M. Richter, N. Dauphas and F.-Z. Teng, *Chemical Geology*, 2009, **258**, 92-103.
43. A. Rodríguez-Navarro and F. Rubio, *Journal of Experimental Botany*, 2006, **57**, 1149-1160.
44. B. P. Pedersen, M. J. Buch-Pedersen, J. P. Morth, M. G. Palmgren and P. Nissen, *Nature*, 2007, **450**, 1111.
45. W. Li, *Acta Geochimica*, 2017, 1-5.
46. Q. L, C. J, B. S and D. D, presented in part at the Goldschmidt Conference, Sacramento, 2014.
47. J. Skulan, D. J. DePaolo and T. L. Owens, *Geochimica et Cosmochimica Acta*, 1997, **61**, 2505-2510.
48. W. Holmes and E. M. Donaldson, *Fish physiology*, 1969, **1**, 1-89.
49. M. Berglund and M. Weiser, *Pure and Applied Chemistry*, 2011, **83**, 397-410.
50. M. E. Wieser, N. Holden, T. B. Coplen, J. K. Boehlke, M. Berglund, W. A. Brand, P. De Bievre, M. Groening, R. D. Loss, J. Meija, T. Hirata, T. Prohaska, R. Schoenberg, G. O'Connor, T. Walczyk, S. Yoneda and X.-K. Zhu, *Pure and Applied Chemistry*, 2013, **85**, 1047-1078.
51. M. O. Naumenko, K. Mezger, T. F. Nägler and I. M. Villa, *Geochimica et cosmochimica acta*, 2013, **122**, 353-362.
52. R. L. Rudnick and S. Gao, in *Treatise on Geochemistry*, ed. H. D. H. K. Turekian, Pergamon, Oxford, 2003, DOI: http://dx.doi.org/10.1016/B0-08-043751-6/03016-4, pp. 1-64.
53. R. D. Beckinsale and N. H. Gale, *Earth and Planetary Science Letters*, 1969, **6**, 289-294.

View Article Online
DOI: 10.1039/C7JA00257B

54. M. A. Grau and C. A. Grau, *Applied Radiation and Isotopes*, 2002, **56**, 153-156.
55. K. Kossert and E. Gunther, *Applied Radiation and Isotopes*, 2004, **60**, 459-464.
56. R. H. Steiger and E. Jäger, *Earth and Planetary Science Letters*, 1977, **36**, 359-362.
57. D. Phillips and E. Matchan, *Geochimica et Cosmochimica Acta*, 2013, **121**, 229-239.

View Article Online
DOI: 10.1039/C7JA00257B

Potassium isotopic compositions measured by MC-ICP-MS in cold-plasma, high-resolution mode indicate terrestrial variability in $^{41}K/^{39}K$ ratios.

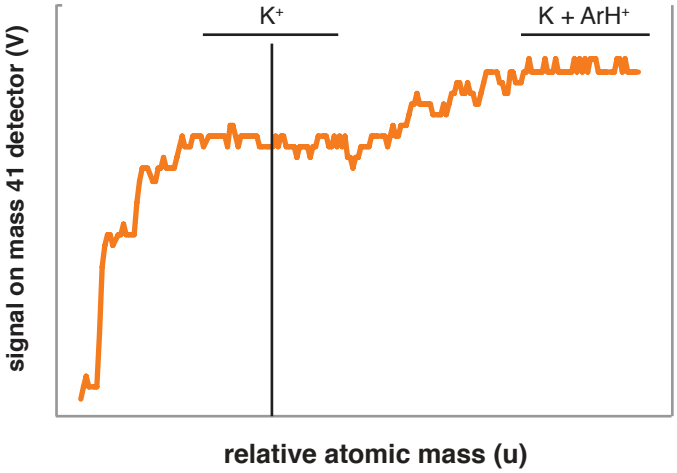

Table 1. NEPTUNE Plus Instrument Settings

Introduction system	Quartz spray chamber, APEX desolvating nebulizer
Cones	standard nickel
Sample gas flow	0.95-1.40 L/min
Cooling gas flow	18 L/min
Auxiliary gas flow	0.6-0.7 L/min
RF Power	500-600 W
Cup configuration	L3 (mass 39), Ax (mass 40), H1 (mass 41)
Focus	160
Shape	165 - 190
Z position	- 0.6 to 1.3

View Article Online
DOI: 10.1039/C7JA00257B

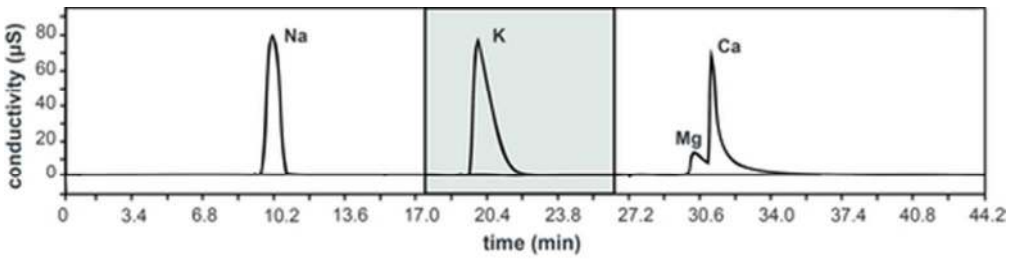

43x10mm (300 x 300 DPI)

View Article Online
DOI: 10.1039/C7JA00257B

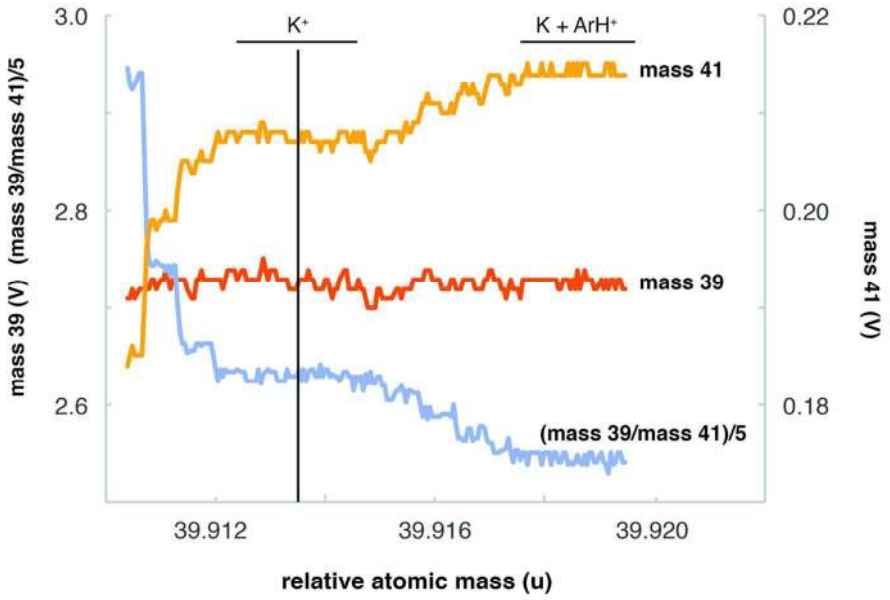

118x94mm (300 x 300 DPI)

View Article Online
DOI: 10.1039/C7JA00257B

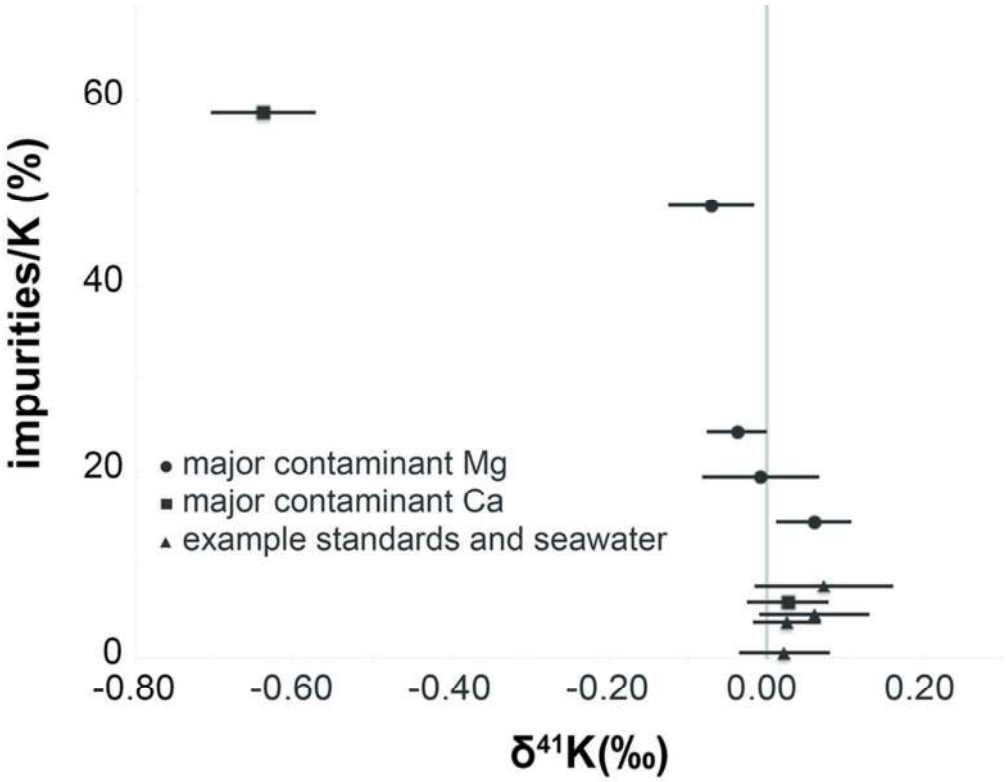

75x58mm (300 x 300 DPI)

View Article Online
DOI: 10.1039/C7JA00257B

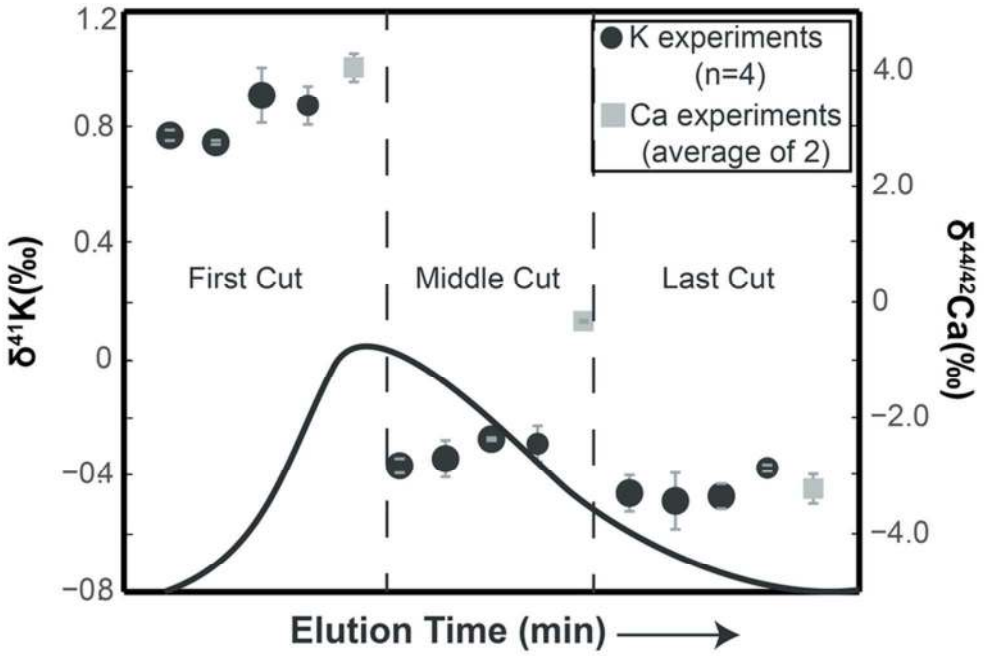

75x49mm (300 x 300 DPI)

View Article Online
DOI: 10.1039/C7JA00257B

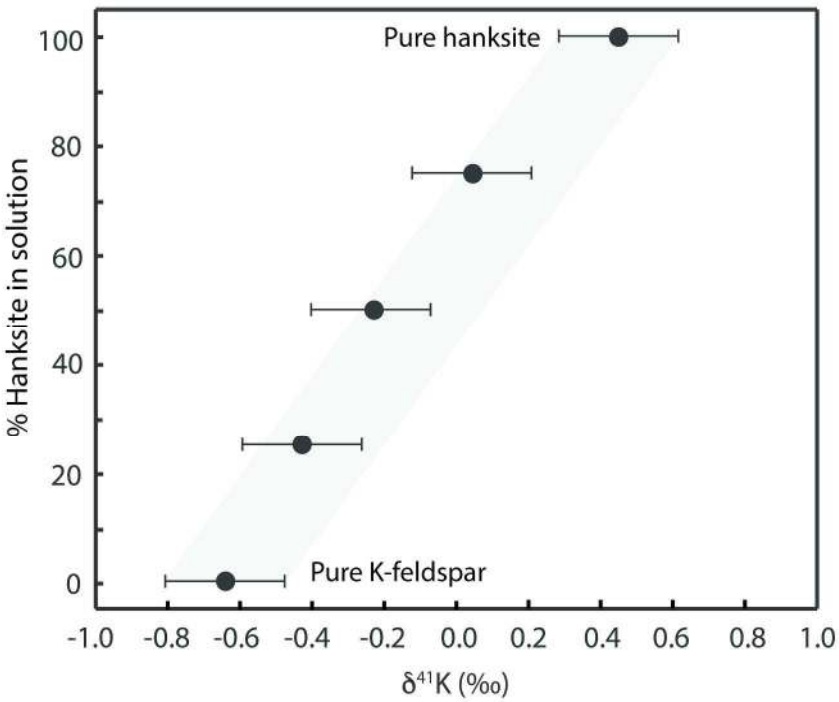

211x273mm (300 x 300 DPI)

View Article Online
DOI: 10.1039/C7JA00257B

199x199mm (300 x 300 DPI)

View Article Online
DOI: 10.1039/C7JA00257B

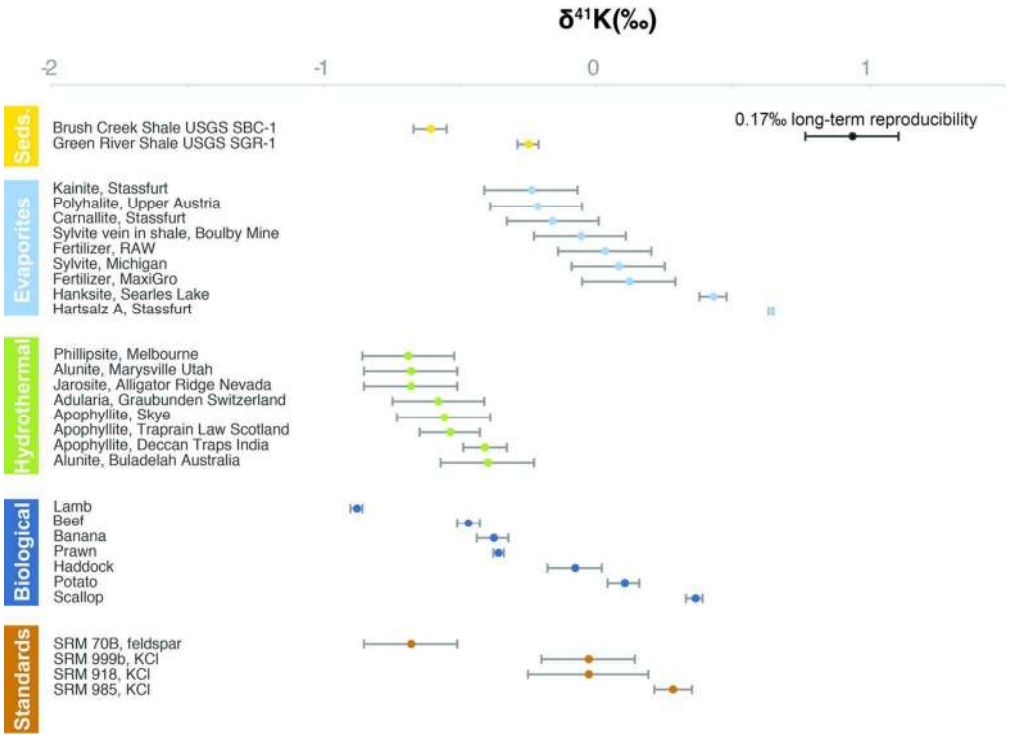

119x87mm (300 x 300 DPI)

View Article Online
DOI: 10.1039/C7JA00257B

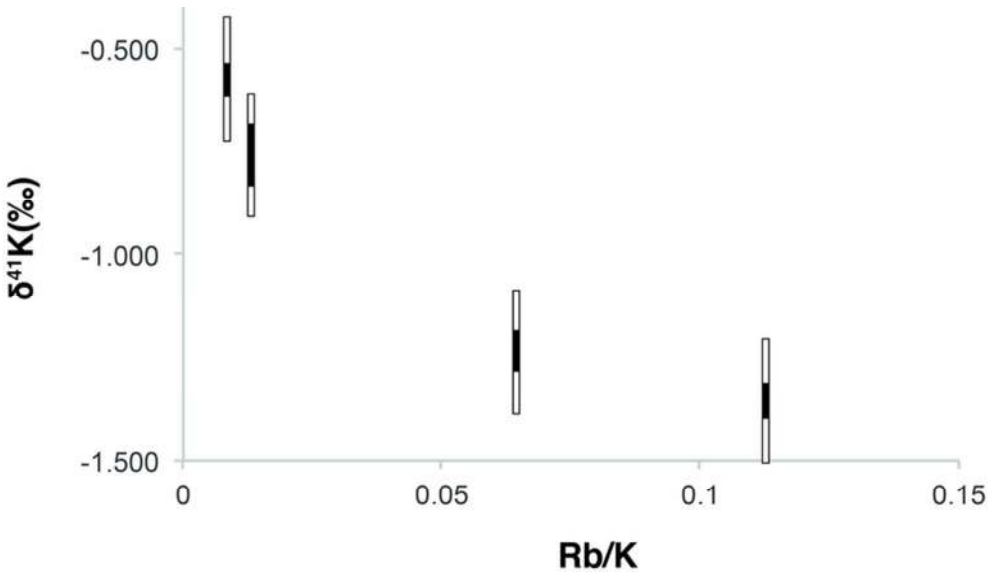

73x42mm (300 x 300 DPI)

View Article Online
DOI: 10.1039/C7JA00257B

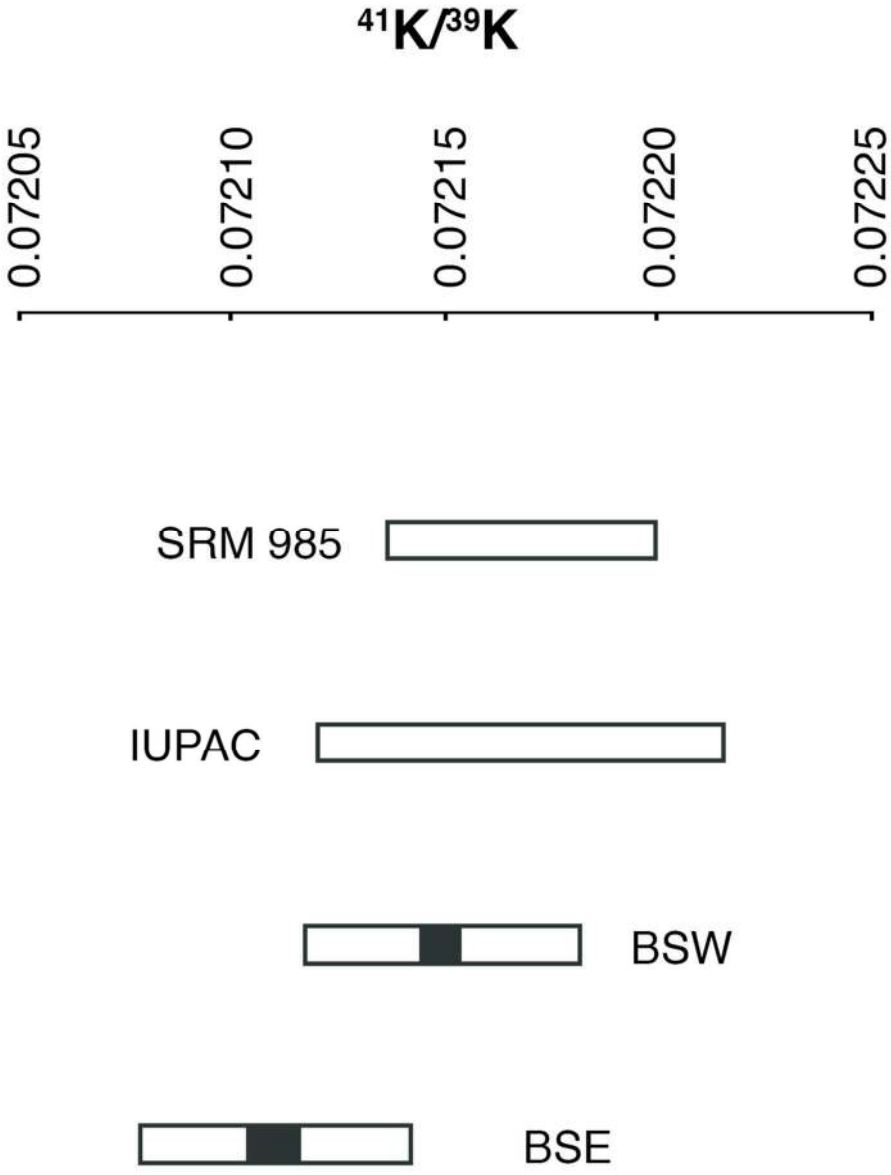

94x125mm (300 x 300 DPI)